Fisher, A., Davis, E.E., and Escutia, C. (Eds.), 2000
Proceedings of the Ocean Drilling Program, Scientific Results, Vol. 168

8. CALCIUM CARBONATE STABILITY IN THE SEDIMENTS OF THE EASTERN FLANK OF THE JUAN DE FUCA RIDGE[1]

Christophe Monnin,[2] Anne-Marie Karpoff,[3] and Martine Buatier[4]

ABSTRACT

Thermodynamic calculations were used to investigate the calcite and aragonite saturation states of sediment pore waters collected during Ocean Drilling program (ODP) Leg 168 on the eastern flank of the Juan de Fuca Ridge. An aqueous carbonate model was used, based on apparent stability constants designed for standard seawater at oceanic conditions, which is the base of the computer program CO2SYS. We discuss possible biases that may result from the application of such models to oceanic sediment pore waters that are slightly altered seawater where calcium has replaced magnesium.

The geochemistry of calcium carbonates at the top of the sediment column at all sites except Sites 1030 and 1031 is dominated by the diagenetic production of alkalinity and subsequent calcium carbonate precipitation. Our calculations show that no calcium carbonate mineral is at equilibrium with the pore waters at the shipboard conditions (20°C, 1 bar). The scatter in the analytical data (especially pH) for pore-water compositions does not allow us to distinguish between calcite and aragonite. At Sites 1023–1029 and 1032, the saturation indices of calcium carbonate minerals calculated for the in situ temperatures and pressures increase with depth from close to equilibrium values at the seafloor to an almost constant supersaturation at depth as indicated by an affinity of the dissolution reaction around 2 kJ/mol. At colder sites, there is a return to equilibrium near the sediment/basement interface, whereas at all other sites (except Sites 1030 and 1031) supersaturation is maintained down to basement. The decrease in pore-water strontium concentration in the first few tens of meters of sedimentary cover can be explained by an uptake of Sr resulting from calcite precipitation, which is consistent with our calculations, but not with the commonly observed increase in pore-water Sr concentration caused by recrystallization of biogenic calcium carbonates. At greater depth in the sediment column, the variation in pore-water Sr concentration is complex and cannot be explained solely by calcium carbonate precipitation. At all sites, the pore-water Mg/Ca ratio displays variations similar to the Sr/Ca ratio.

Sites 1030 and 1031 display a diffuse fluid discharge. Pore waters are at equilibrium in the lower half of the sediment column at Site 1030. Site 1031 shows equilibrium throughout nearly the entire sediment column, except for the topmost section where slight supersaturation is found. The tendency toward chemical equilibrium at these two sites results from competition between the advection of a low-alkalinity, upwelling basement fluid and alkalinity production by organic matter oxidation.

INTRODUCTION

Massive fluid flow through oceanic ridge flanks is responsible for a large part of the heat loss of the oceanic crust and likely plays a major role in the geochemical cycling of chemical elements (Wolery and Sleep, 1976; Stein et al., 1995; Kadko et al., 1995; Elderfield and Schultz, 1995). Leg 168 was designed to study the characteristics of fluid circulation in the eastern flank of the Juan de Fuca Ridge (northeast Pacific). A series of ten holes were drilled through the sediments and into the upper basaltic basement along an east-west transect (Fig. 1). Data collected during Leg 168 provide evidence that fluid circulation is still active 100 km from the ridge axis (Davis, Fisher, Firth, et al., 1997).

Both diffuse and focused fluid discharge to the deep ocean have been found on the eastern flank of the Juan de Fuca Ridge. A diffuse vertical upwelling of basement fluid occurs at Sites 1030 and 1031 where the sediment layer is only 40–50 m thick. Diffuse flow in this area was documented from heat-flow data and pore-water compositions from shallow cores (Wheat and Mottl, 1994). Fluid discharge from basement took place during drilling at Site 1026 after penetration of the sediment layers and showed that basement at this location is overpressured, but the sediments were thick enough (250 m) to prevent seepage at the seafloor (Davis, Fisher, Firth, et al., 1997; Fisher et al., 1997). A submarine spring producing warm (25°C) waters was discovered during *Alvin* dives in August 1995 at the top of an isolated basaltic outcrop called Baby Bare (Mottl et al., 1998). Site 1026 is located a few kilometers north of Baby Bare.

The estimate of chemical fluxes originating from fluid circulation in oceanic ridge flanks is difficult because of the paucity of the data and the large range of crustal conditions (Mottl and Wheat, 1994; Elderfield and Schultz, 1995; Kadko et al., 1995). Sansone et al. (1998) evaluated the contribution of the low-temperature hydrothermal alteration of the oceanic crust to the global carbon budget from the composition of the Baby Bare spring waters. In this paper we investigate the stability of calcium carbonates in the sediments of the eastern flank of the Juan de Fuca Ridge from the pore-water compositions using simple thermodynamic calculations.

CALCULATION OF THE CALCIUM CARBONATE SATURATION INDEX FROM THE PORE-WATER COMPOSITIONS

The tendency of calcium carbonate to precipitate can be inferred from simple mass balance calculations applied to the composition of sediment pore waters. For example, it has been shown for Hydrothermal Transition Sites 1023, 1024, and 1025 (Davis, Fisher, Firth, et al., 1997) that the increase in alkalinity in sediment pore waters is lower than the decrease in sulfate concentration expected from the stoichiometry of the reaction of organic matter oxidation:

$$2CH_2O + SO_4^{2-}(aq) = 2HCO_3^-(aq) + H_2S(g). \quad (1)$$

[1]Fisher, A., Davis, E.E., and Escutia, C. (Eds.), 2000. *Proc. ODP, Sci. Results,* 168: College Station TX (Ocean Drilling Program).

[2]CNRS/Université Paul Sabatier, Laboratoire de Géochimie, 38 rue des Trente Six Ponts, 31400 Toulouse, France. monnin@lucid.ups-tlse.fr

[3]CNRS/Université Louis Pasteur, Centre de Géochimie de la Surface, 1 rue Blessig, 87084 Strasbourg, France.

[4]Université de Franche-Comté, Laboratoire de Géosciences, 16 route de Gray, 25030 Besançon, France.

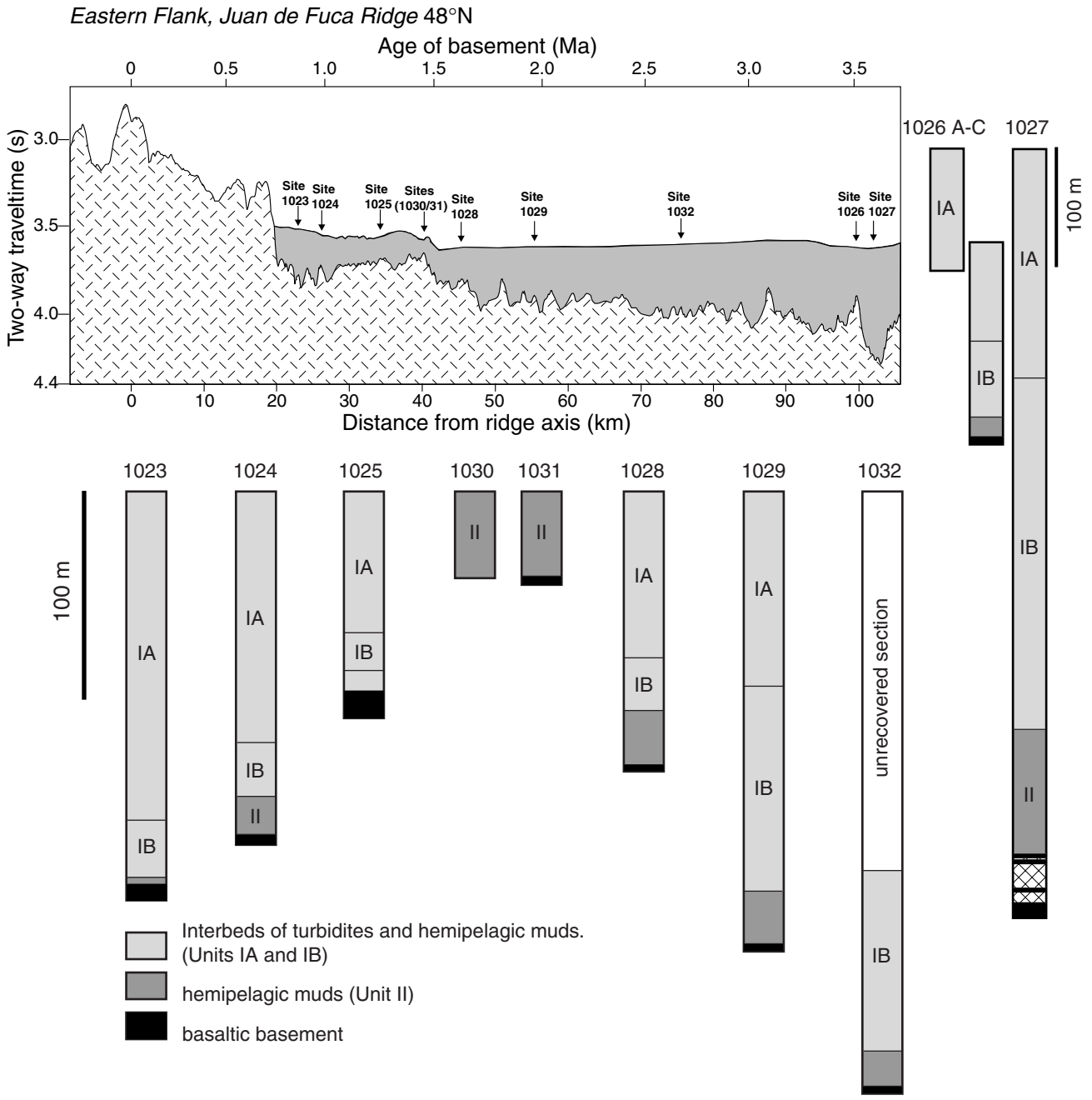

Figure 1. Basement topography and sedimentary cover of the eastern flank of the Juan de Fuca Ridge and synthetic lithologic sections of the drilled Sites 1023–1032.

This low alkalinity increase is attributed to calcium carbonate precipitation. Thermodynamic calculations allow temperature, pressure, and solution composition to be combined into a single parameter (mineral saturation indices or free energies of reaction) to determine the mineral-solution reactions likely to control the composition of interstitial fluids.

The thermodynamics of the carbonate system in the ocean has been given very wide attention because of the primary importance of the carbon budget on global geochemical cycles. A computer program called CO2SYS was developed to calculate inorganic carbon speciation in seawater (Lewis and Wallace, 1999). The code allows the user to choose between different pH scales. It incorporates various models and formulations of the thermodynamic constants for the carbonate system. An important feature of the CO2SYS development is that the authors have crosschecked the relevant primary literature and corrected errors found in articles.

Almost all aqueous carbon dioxide models included in CO2SYS rely on a description of the CO_2 system based on apparent stability constants measured in standard seawater as a function of temperature, pressure, and salinity at oceanic conditions (i.e., at temperatures from –1° to ~40°C, pressures to 1000 bars, and salinities to 40‰). In situ pressures in the Leg 168 sediments are hydrostatic and around 300 bars, but temperatures can reach 63°C. Calculations using CO2SYS above 40°C require that the expressions for the apparent constants for the carbonate system and for calcium carbonates be extrapolated beyond their intended range of application. Also, although

measured salinities are close to 35‰, sediment pore waters collected during Leg 168 are not standard seawater; they are depleted in Mg and enriched in Ca (Davis, Fisher, Firth, et al., 1997). We assume that composition changes implied by the replacement of Mg by Ca do not induce large changes in the thermodynamic properties of the aqueous solution.

The saturation state of the pore waters with respect to calcium carbonates can be inferred from the values of the calcite and aragonite saturation indices at in situ temperature and pressure. The calcium carbonate apparent ionic product (Q^*) is the product of the measured calcium concentration by the carbonate concentration calculated from measured pH and alkalinity values

$$Q^* = m_{Ca^{2+},\,aq} \cdot m_{CO_3^{2-},\,aq}, \quad (2)$$

in which m is the molality of the designated species. The saturation index (SI) is defined as the ratio of the calcium carbonate apparent ionic product to the apparent solubility product of the considered solid (calcite or aragonite)

$$\mathrm{SI} = \frac{Q^*}{K^*_{sp}}. \quad (3)$$

The SI is related to the free energy (or chemical affinity, A) of the dissolution reaction of the considered mineral by

$$A = RT\left[\log\frac{Q^*}{K^*_{sp}}\right], \quad (4)$$

where R is the gas constant and T the absolute temperature. The solution is undersaturated when A is negative (minerals can dissolve) and supersaturated for positive values (minerals can precipitate). Using the free energy of reaction instead of the saturation index expands the undersaturated side of the plotted data and reduces the supersaturation side (Figs. 2–3).

Values of the affinity of the dissolution reaction are always greater for calcite than for aragonite (Fig. 3). This reflects the greater stability of calcite when compared to that of aragonite: the driving force for dissolution is greater for aragonite, and the driving force for precipitation is larger for calcite. This is one cause of the well-known recrystallization of calcium carbonate: dissolution of aragonite and precipitation of calcite. The difference between the affinities of reaction for calcite and aragonite are small (about 0.4 kJ/mol) compared to the scatter of the data depicted in Figure 3. It is impossible to distinguish between calcite and aragonite at this level of accuracy.

Because pH on board the ship was measured on the NBS pH scale, we retained this option throughout all this work. Data plotted in Figure 3 shows that pore-water pH values are scattered over a range that can reach up to 0.5 pH units. A few samples of the sediment from Leg 168 were squeezed to extract the pore waters 4 hr after core recovery (the so-called "post-MST" samples in table 16 of Davis, Fisher, Firth, et al., 1997), whereas the usual procedure was to process the samples in the chemistry lab immediately after recovery (i.e., within an hour). The difference in pH and alkalinity of these samples with those squeezed right after recovery is small but noticeable. This pH difference is comparable to the pH scatter of the whole data set, but alkalinity is lower, indicating active calcium carbonate precipitation within the samples following recovery. This sampling artifact contributes to the scatter in the pH data (Fig. 3). We calculated the distribution of carbonate species for the laboratory pressure and temperature at which the pH and alkalinity determinations were made, as well as for in situ conditions to verify that late analysis does not lead to major changes in the affinity of reaction. We checked that neither calcite nor aragonite are at equilibrium with the pore waters at the shipboard conditions (20°C and 1 bar). Results indicate that pore waters are largely supersaturated at these conditions.

We used the composition of the Baby Bare spring water (Mottl et al., 1998) to calculate the variation of the affinity of the calcite dissolution reaction implied by the use of different aqueous carbon dioxide models (Lewis and Wallace, 1999). Figure 2 shows that the results obtained with these various models are quite consistent (within 0.1 kJ/mol of each other) up to a temperature of about 30°C. Beyond this temperature, the "Geosecs" model leads to an unrealistic trend in the affinity of reaction. Other models are consistent within 0.2 kJ/mol up to about 60°C and show smooth variations of the affinity of reaction with temperature, as can be expected. We retained the "Dickson and Millero" option throughout this work. In these calculations we assume that pH does not change with temperature. Figure 2 also shows that the supersaturation of the Baby Bare spring waters with respect to calcite decreases when temperature decreases. These waters are venting to the deep ocean at 25°C, having cooled from an estimated temperature of 64°C during their ascent (Sansone et al., 1998). Our calculations are consistent with the removal of carbon from the spring waters by active calcium carbonate precipitation in the igneous basement at temperatures higher than that of the venting fluids, as concluded by Sansone et al. (1998).

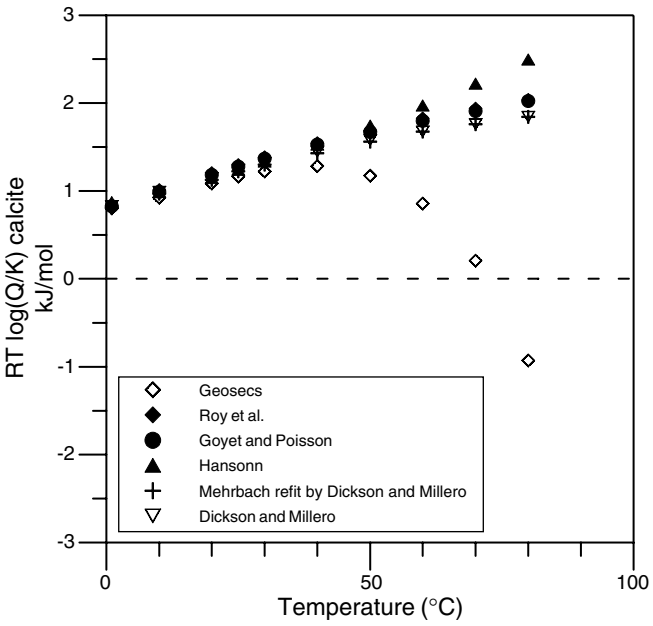

Figure 2. The affinity of the calcite dissolution reaction of the Baby Bare spring water (Mottl et al., 1998) for rounded values of temperature and for different aqueous calcium carbonate models included in the CO2SYS code (see the program's user guide for a full description of the models).

CALCIUM CARBONATE STABILITY IN THE JUAN DE FUCA EASTERN FLANK SEDIMENTS

Figure 3 shows pH, alkalinity (Davis, Fisher, Firth, et al., 1997), the free energy of calcium carbonate dissolution, the Sr content, and the Mg/Ca and Sr/Ca ratios of the pore waters for Sites 1023–1031. Magnesium and strontium are common substitutes for calcium in calcium carbonates. The calcium data is the shipboard data (Davis, Fisher, Firth, et al., 1997). The Sr concentrations have been measured in Toulouse by inductively coupled plasma-mass spectrometer (ICP-MS) using Indium as an internal standard (Freydier et al., 1995) and are reported elsewhere (Mottl et al., Chap. 8, this volume). We correlate the behavior of Mg and Sr in pore waters to the calcium carbonate saturation state of the pore waters inferred from our calculations.

It can be seen in Figure 3 that most of the pore waters are supersaturated with respect to both calcite and aragonite. At all sites, the reaction affinity increases from close to equilibrium values at the seafloor and reaches an almost constant value at depth of 2–3 kJ/mol.

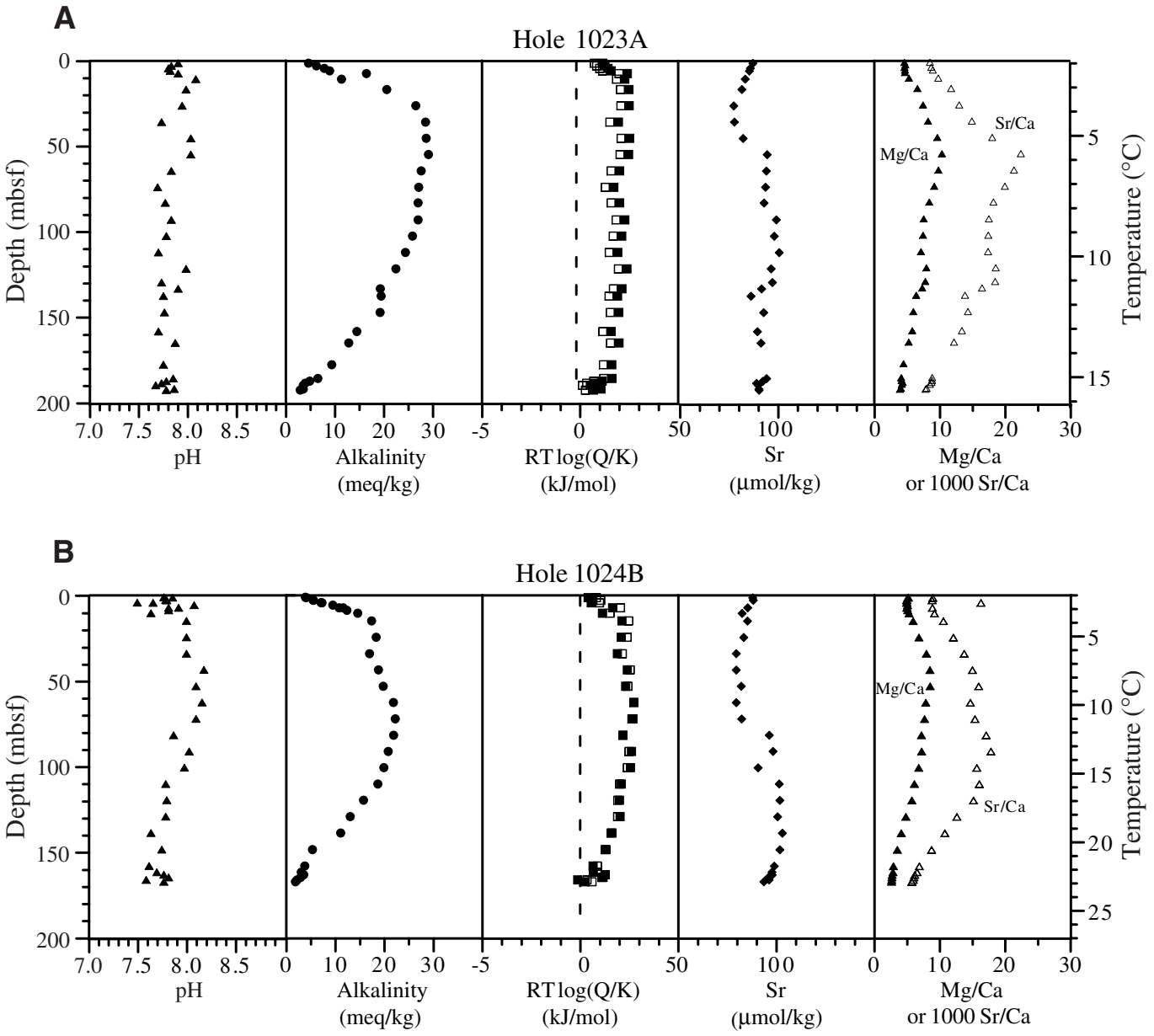

Figure 3. pH, alkalinity, the affinity of calcite (solid squares) and aragonite (open squares) dissolution reactions, strontium concentration, and the Mg/Ca and Sr/Ca ratios vs. depth for Sites 1023–1032. The dashed vertical line denotes equilibrium. **A.** Hole 1023A. **B.** Hole 1024B. **C.** Hole 1025B. **D.** Holes 1026A and 1026C; note the change in scale for the strontium concentration. **E.** Hole 1027B. **F.** Hole 1028A. **G.** Hole 1029A. **H.** Hole 1030A. **I.** Hole 1031A. **J.** Hole 1032A.

Pore-water calcium (Davis, Fisher, Firth, et al., 1997) and strontium (Mottl et al., Chap. 8, this volume) concentrations decrease in the first 10–20 mbsf. In general, the strontium concentration in interstitial waters of marine sediments increases as the result of calcium carbonate recrystallization (Morse and Mackenzie, 1990, p. 402; Elderfield et al., 1982; Oyun et al., 1995) in accordance with

$$Ca_{1-x}Sr_xCO_3(s) + (y-x)Ca^{2+}(aq), \quad (5)$$
$$= Ca_{1-y}Sr_yCO_3(s) + (y-x)Sr^{2+}(aq)$$

in which y > x. The reaction represented by Equation 5 consumes calcium from the pore water and releases strontium to it, hence increasing the Sr/Ca ratio of the aqueous phase. This has been shown (Elderfield et al., 1982; Oyun et al. 1995) for sites where pore-water sampling was not as detailed as that of Leg 168. For example, Elderfield et al. (1982) used sediment and pore-water composition data for DSDP Sites 288 and 289 for which only two samples have been collected in the upper 100 mbsf. During Leg 168, five samples were collected in the first and last cores (first 10 m and last core above basement) and then at least one sample in each core in between. Faure and Powell (1972, p. 79) report that "precipitation of calcite from a solution containing Sr^{2+} will increase the Sr/Ca ratio of the aqueous phase, while precipitation of aragonite at temperatures below 50°C will decrease this ratio." The Sr/Ca ratio of the aqueous phase in Leg 168 pore waters increases downhole from the seafloor (Fig. 3), consistent with this assertion. Sr substitution for Ca in calcite can explain the decrease in the pore-water Sr concentration in the first tens of meters of the sedimentary column from the seawater value of 89 µmol/kg at the seafloor. This requires that there is no dissolution and subsequent recrystallization of biogenic carbonates.

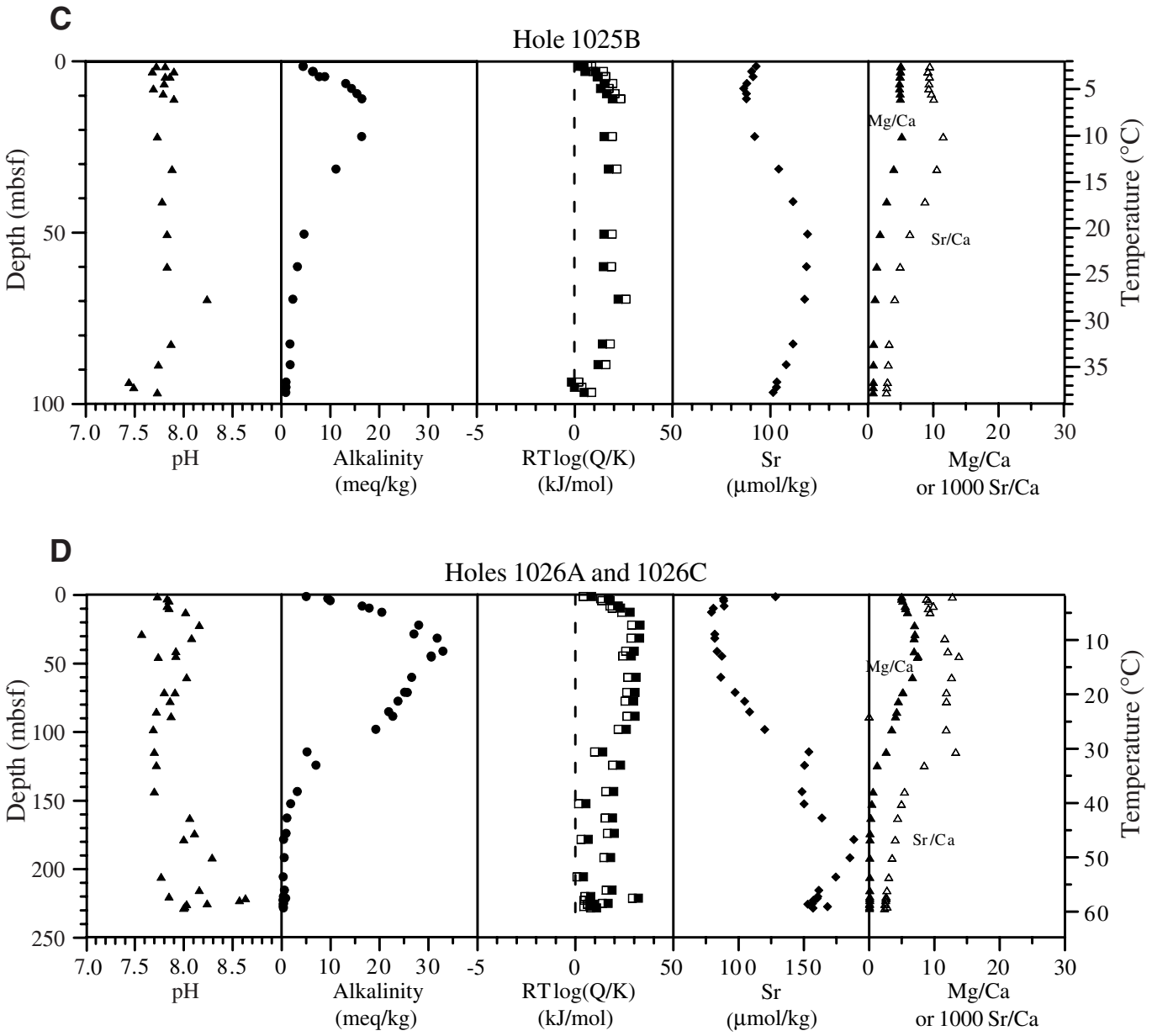

Figure 3 (continued).

The Hydrothermal Transition Transect—Sites 1023, 1024, and 1025

At Sites 1023, 1024, and 1025, the affinity of the calcite dissolution reaction increases to about 3 kJ/mol and then decreases to reach values close to equilibrium near basement (Fig. 3). It is interesting to note that, at Sites 1024 and 1025, the deepest points are on the equilibrium line. Sr is almost constant at Site 1023 (Fig. 3) and only increases slightly at Site 1024 (Fig. 3B), whereas its value reaches 110 µmol/kg before returning to modern seawater values at Site 1025 (Fig. 3C). It can be also noticed that, at Sites 1023 and 1024, alkalinity reaches its maximum value at a depth where sulfate begins to be totally depleted in the pore waters. It also coincides with the onset of methane production, which occurs at about 50 mbsf at Sites 1023 and 1024 (Davis, Fisher, Firth, et al., 1997). One can see in Figure 3 that the alkalinity maximum is also concomitant with a marked change in the pore-water Mg/Ca and Sr/Ca ratios at Sites 1023 and 1024. These ratios are almost constant at Site 1025 before decreasing below a depth of 20 mbsf. There is no methanogenesis at Site 1025.

The Rough Basement Transect—Sites 1026 and 1027

In Leg 168 sites, the warmest temperatures have been found at Sites 1026 and 1027, around 63°C, at the sediment/basement interface (Davis, Fisher, Firth, et al., 1997). This temperature homogenization is attributed to the vigor of fluid circulation within the basement. At Site 1026, there is an increase in the affinity of reaction to about 3 kJ/mol, then a decrease to lower values scattered between 0 and 2 kJ below 150 mbsf (Fig. 3D). There is a marked increase in the scatter of the pH data below 130–150 mbsf as well as a trend to higher values (Fig. 3D). This change can also be seen in the Sr data, which show a local maximum at this depth (130 mbsf). The strontium concentration in pore waters reaches 170 µmol/kg before decreasing again when basement is approached (Fig. 3D). Despite this complex

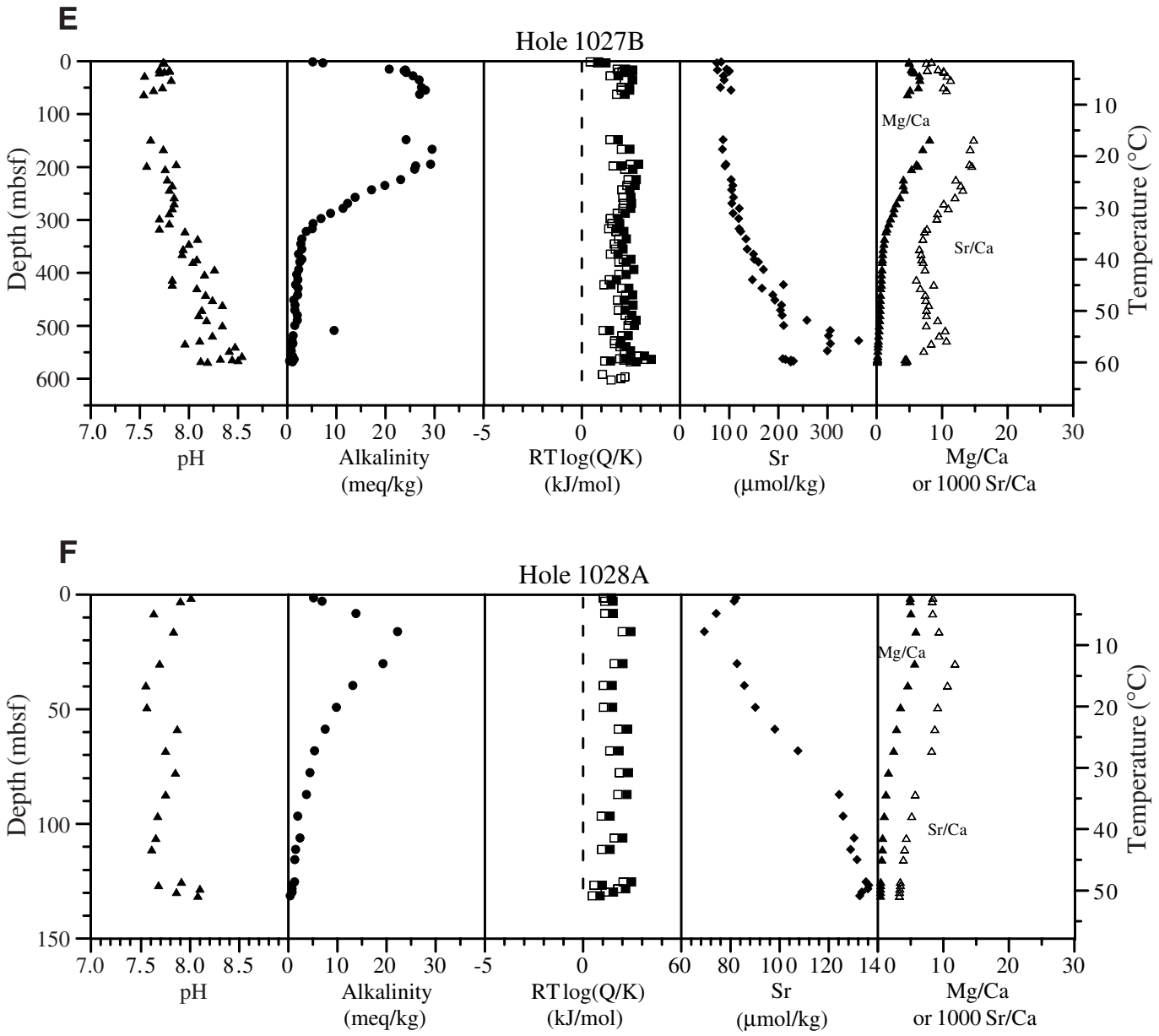

Figure 3 (continued).

variation in Sr concentration with depth, the Mg/Ca and Sr/Ca ratios at Site 1026 resemble those found for the Hydrothermal Transition sites.

At Site 1027 (Fig. 3E) pore waters remain supersaturated down to basement. This is consistent with the massive calcium carbonate occurrence in veins crosscutting basement rocks at this location. Only one example of such calcite-containing veins has been found at Site 1026 (Davis, Fisher, Firth, et al., 1997, p. 128). At Site 1027, the strontium concentration increases to very large values (~360 µmol/kg) before displaying a large decreasing gradient near basement.

The Buried Basement Transect—Sites 1028, 1029, 1030, 1031 and 1032

Pore-water chemical results from Sites 1028 and 1029 are similar (Fig. 3F, G) with the affinity of reaction being 1–2 kJ/mol throughout the sediment column. At Site 1028 (Fig. 3F), Sr first decreases, then increases to about 135 µmol/kg, and then decreases again close to basement.

At Site 1029, the variation in strontium concentration with depth (Fig. 3G) shows the same complexity as that at Site 1026 (Fig. 3E). There is also a marked reversal in the Sr behavior near basement. The Mg/Ca and Sr/Ca values at this site resemble those found at other sites: an almost linear increase from the seafloor and then a sharp reversal toward low values at depth.

Sediment cores were retrieved at Site 1032 from 195 mbsf to basement at 285 mbsf. The data depicted in Figure 3I show that there is a large scatter in pH at depth. This pH variation leads to reaction affinities between 0.5 and 2 kJ/mol, which may be a little bit lower than was found in deeper sediment sections of other Leg 168 sites.

At Sites 1030 and 1031, which are located above a basaltic outcrop buried under 40–50 m of sediments, upwelling of basement fluid through the sediment cover has been identified by the characteristic shape of the pore-water concentration profiles of elements, especially magnesium and chlorinity (Davis, Fisher, Firth, et al., 1997). Strontium displays such a behavior: its concentration increases from the seawater values (89 µmol/kg) and then reaches a constant value of 110 µmol/kg at Site 1030 and 111 µmol/kg at Site 1031 (Fig. 3H, I).

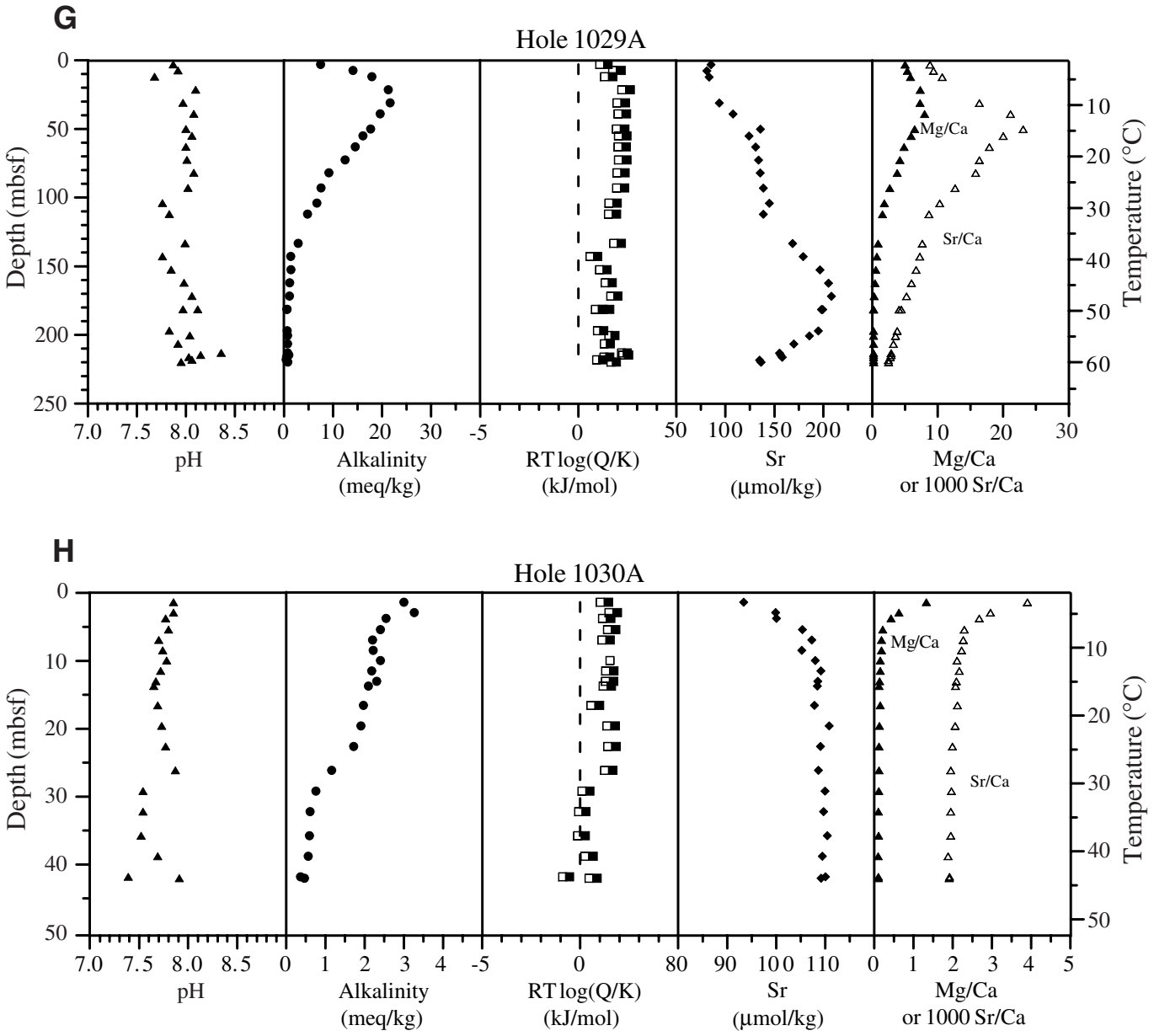

Figure 3 (continued).

These values are similar to the strontium concentration of the Baby Bare spring fluid (110 µmol/kg; Mottl et al., 1998) and of the basement fluid sampled with the downhole water sampler temperature probe (WSTP; Fisher et al., 1997) at Hole 1026B (111 µmol/kg, Mottl et al., Chap. 8, this volume). Whereas alkalinity generally increases downhole as a result of bacterial sulfate reduction at other Leg 168 sites, it continuously decreases at Sites 1030 and 1031 to very low values that are also comparable to the alkalinity of the Baby Bare spring fluids (Fig. 3H, I). The effects of diagenetic reactions like the decrease in sulfate and the alkalinity production are masked by the upwelling fluid. Because the rate of advection is faster at Site 1031 than at Site 1030, alkalinity at Site 1030 is higher than at Site 1031 (Davis, Fisher, Firth, et al., 1997). Calcite or aragonite are at equilibrium with the pore waters from basement at 45 mbsf up to a depth of 30 mbsf, where the pore waters become supersaturated up to the seafloor (Fig. 3H). Equilibrium between pore waters and calcium carbonate is reached at Site 1031 in almost the entire sediment column, with a trend to slight undersaturation just below the seafloor (Fig. 3I). These two sites are the only ones among the Leg 168 sites where frequent dissolution of foraminifers and coccolith tests have been observed by scanning electronic microscopy (Buatier et al., in press). This is also consistent with micropaleontological observations (X. Su, unpubl. data). Carbonate dissolution is linked to smectite and zeolite formation in altered layers of the sediment (Buatier et al., in press). There is a slight change in the Sr concentration (Fig. 3I) for the last two samples near the sediment/basement interface where the sediment alteration is most intense (Buatier et al., in press).

For an infinite rate of advection, a fluid upwelling through the sediment cover will reach the seafloor unaltered because the rate of advection is faster than the rate of chemical reactions. Inversely, the fluid would be at equilibrium with calcite for an infinite rate of calcite dissolution or precipitation. At Sites 1030 and 1031 the distribution of alkalinity (and of the affinity of the calcite/aragonite dissolution reaction) is the result of the competition between the rate of fluid advection and the rate of chemical reactions. If we assume that a value of the affinity of reaction of about 2 kJ/mol is representative of calcium carbonate precipitation at most Leg 168 sites (Fig. 3), it takes a longer distance (i.e., sediment thickness) to reach this representative

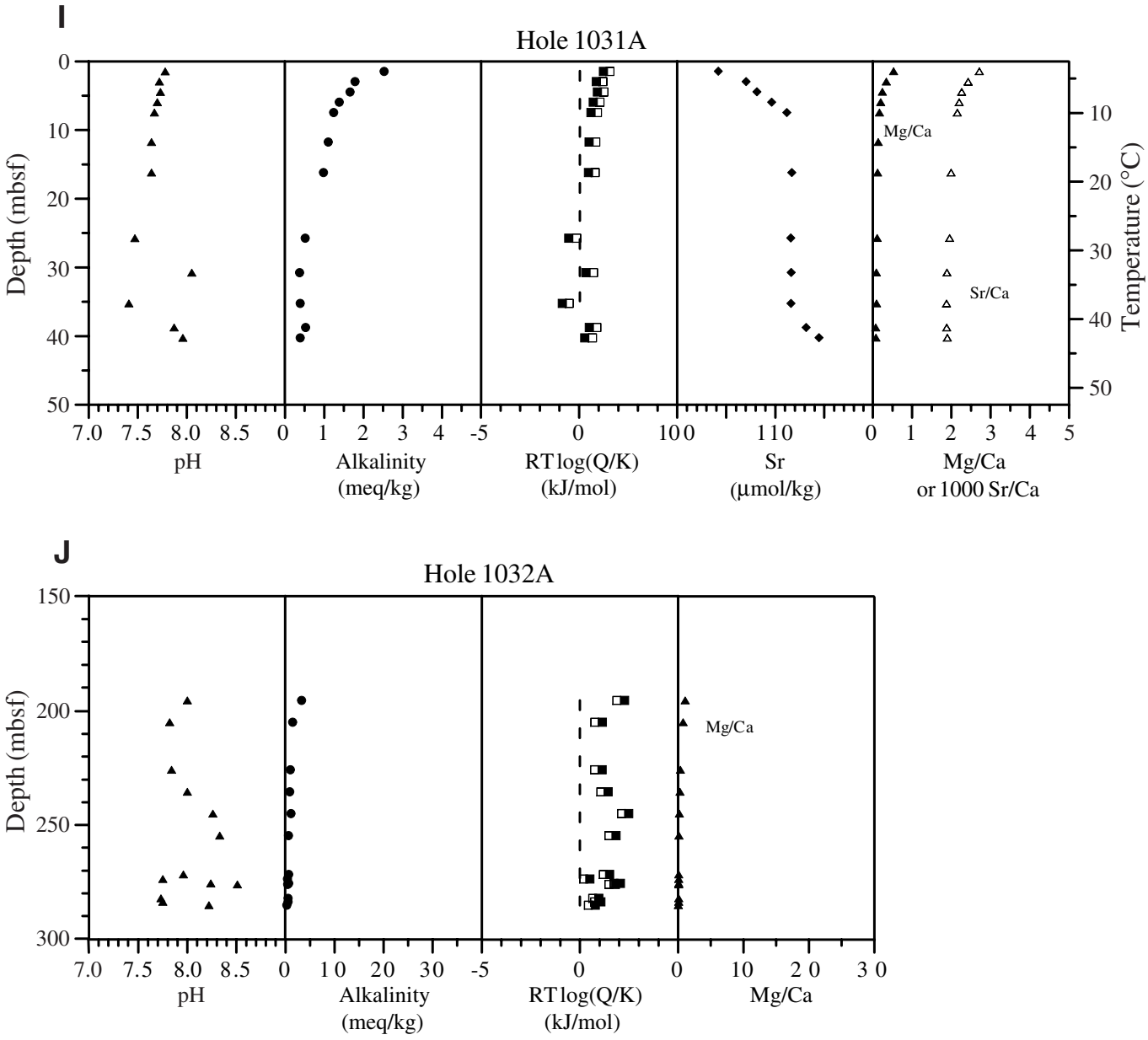

Figure 3 (continued).

value in the case of a rapidly advecting fluid at Site 1031 than in the case of the slower fluid at Site 1030 (Fig. 3H, I).

Several processes can lead to calcium carbonate supersaturation, which can result from the inhibition of precipitation. This can be due to the poisoning of reactive surfaces by organic matter. It is also well known that magnesium and orthophosphate are inhibitors of calcite precipitation. It is interesting to note that organic matter oxidation provides the needed reactant (alkalinity) for calcium carbonate formation at the same time that it provides phosphate to the pore water. A detailed study of the mechanisms of calcium carbonate formation in the sediments of the eastern flank of the Juan de Fuca Ridge is needed to elucidate the problem.

CONCLUSIONS

Thermodynamic calculations indicate that most of the pore waters of Leg 168 sediment are supersaturated with calcite and aragonite, with an affinity of reaction around 2 kJ/mol. At colder sites (i.e., the HT sites), there is a return to equilibrium with calcium carbonate at the sediment/basement interface. Calcium carbonate geochemistry at the top of the sediment column at all but Sites 1030 and 1031 is dominated by the diagenetic production of alkalinity and subsequent calcite precipitation.

The decrease in pore-water Sr concentration in the first few tens of meters of the sedimentary cover can be explained by an uptake of Sr by calcite precipitation, but is not consistent with the commonly observed increase in pore-water Sr concentration resulting from the recrystallization of biogenic calcium carbonates. At greater depth in the sediment column, the variation in pore-water Sr concentration is very complex and cannot be explained solely by calcium carbonate precipitation.

At Sites 1030 and 1031, where a diffuse fluid discharge takes place, pore waters are at equilibrium with calcite or aragonite in the lower half of the sediments at Site 1030 and throughout the sediment

column except near the seafloor at Site 1031. It appears that equilibrium is achieved because the upwelling of a low-alkalinity fluid counterbalances the increase in alkalinity caused by diagenesis.

The scatter in the analytical data for pore-water compositions does not allow distinguishing between calcite and aragonite precipitation being favored, which would be possible for open-ocean water column compositions. This brings some justification to the use of aqueous calcium carbonate models that have been designed for oceanic conditions. For sediment pore waters that are not too different from standard seawater, our calculations provide some insight into calcium carbonate geochemistry in a low-temperature environment of an oceanic ridge flank.

ACKNOWLEDGMENTS

C.M. is very grateful to Andy Dickson for sharing his expertise on the geochemistry of the carbonate system in the ocean and for indicating the existence of the CO2SYS program. The editorial work of Andy Fisher and Gigi Delgado is deeply appreciated. This work has been financially supported by CNRS program Dynamique des Transferts Terrestres.

REFERENCES

Buatier, M., Monnin, C., Früh-Green, G., and Karpoff, A.-M., in press. Fluid-sediment interactions related to hydrothermal circulation in the eastern flank of the Juan de Fuca Ridge. *Chem. Geol*.

Davis, E.E., Fisher, A.T., Firth, J.V., et al., 1997. *Proc. ODP, Init. Repts.,* 168: College Station, TX (Ocean Drilling Program).

Elderfield, H., Gieskes, J.M., Baker, P.A., Oldfield, R.K., Hawkesworth, C.J., and Miller, R., 1982. $^{87}Sr/^{86}Sr$ and $^{18}O/^{16}O$ ratios, interstitial water chemistry and diagenesis in deep-sea carbonate sediments of the Ontong-Java Plateau. *Geochim. Cosmochim. Acta,* 46:2259–2268.

Elderfield, H., and Schultz, A., 1995. Mid-ocean ridge hydrothermal fluxes and the chemical composition of the ocean. *Annu. Rev. Earth Planet. Sci.,* 24:191–224.

Faure, G., and Powell, J.L., 1972. *Strontium Isotope Geology:* New York (Springer-Verlag).

Fisher, A.T., Becker, K., and Davis, E.E., 1997. The permeability of young oceanic crust east of Juan de Fuca Ridge determined using borehole thermal measurements. *Geophys. Res. Lett.,* 24:1311–1314.

Freydier, R., Dupre, B., and Polve, M., 1995. Analyses by inductively coupled plasma mass spectrometry of Ba concentrations in water and rock samples: comparison between isotope dilution and external calibration with or without internal standard. *Eur. Mass Spectr.,* 1:283–291.

Kadko, D., Baross, J., and Alt, J., 1995. The magnitude and global implications of hydrothermal flux. *In* Humphris, S.E., et al. (Eds.), *Seafloor Hydrothermal Systems: Physical, Chemical, Biological and Geological Interactions.* Am. Geophys. Union Monogr., 91:446–466.

Lewis, E., and Wallace, D., 1999. CO2SYS: program developed for CO_2 system calculations. Program and user guide available online on the CDIAC (Carbon Dioxyde Information and Analysis Center) web site (http://cdiac.esd.ornl.gov).

Morse, J.W., and Mackenzie, F.T., 1990. *Geochemistry of Sedimentary Carbonates:* Amsterdam (Elsevier).

Mottl, M.J., and Wheat, C.G., 1994. Hydrothermal circulation through mid-ocean ridge flanks: fluxes of heat and magnesium. *Geochim. Cosmochim. Acta,* 58:2225–2238.

Mottl, M.J., Wheat, C.G., Baker, E., Becker, N., Davis, E., Feely, R., Grehan, A., Kadko, D., Lilley, M., Massoth, G., Moyer, C., and Sansone, F., 1998. Warm springs discovered on 3.5 Ma oceanic crust, eastern flank of the Juan de Fuca Ridge. *Geology,* 26:51–54.

Oyun, S., Elderfield, H., and Klinkhammer, G.P., 1995. Strontium isotopes in pore waters of east equatorial Pacific sediments: indicators of seawater advection through oceanic crust and sediments. *In* Pisias, N.G., Mayer, L.A., Janecek, T.R., Palmer-Julson, A., and van Andel, T.H. (Eds.), *Proc. ODP, Sci. Results,* 138: College Station, TX (Ocean Drilling Program), 813–819.

Sansone, F.J., Mottl, M.M., Olson, E.J., Wheat, C.G., and Lilley, M.D., 1998. CO_2-depleted fluids from mid-ocean ridge flank hydrothermal springs. *Geochim. Cosmochim. Acta,* 62:2247–2252.

Stein, C.A., Stein, S., and Pelayo, A.M., 1995. Heat flow and hydrothermal circulation. *In* Humphris, S.E., et al. (Eds.), *Seafloor Hydrothermal Systems: Physical, Chemical, Biological and Geological Interactions.* Am. Geophys. Union Monogr., 91:425–445.

Wheat, C.G., and Mottl, M.G., 1994. Hydrothermal circulation, Juan de Fuca Ridge eastern flank: factors controlling basement water composition. *J. Geophys. Res.,* 99:3067–3080.

Wolery, T.J., and Sleep, N.H., 1976. Hydrothermal circulation and geochemical flux at mid-ocean ridges. *J. Geol.,* 84:249–275.

Date of initial receipt: 21 December 1998
Date of acceptance: 11 November 1999
Ms 168SR-017